THE EFFECT OF CHANGING THE BLADE STIFFNESS ON THE FLAP-LAG-STALL INSTABILITY OF LARGE WIND TURBINES

J.G. Holierhoek
Delft University of Technology, Faculty of Aerospace Engineering
Delft, the Netherlands

Abstract

One of the instabilities large wind turbines can suffer from is the so-called flap-lag-stall instability. This is caused by the first flap and lead-lag frequencies of the large blade coming closer together as an effect from scaling, combined with the effect of stall. Another instability that can occur in wind turbines operating in or close to stall is an instability due to negative in-plane damping by the aerodynamic forces. To further investigate the effect of the frequencies on the flap-lag-stall instability a blade is simulated using different values for the stiffness in flap and lead lag direction. Bringing these two closer together should decrease the damping when operating close to stall if the blade suffers from the flap-lag-stall instability. Simulations have been performed on five different blades, a baseline and four with a reduction in the difference between the first flap and first lag frequency. From these simulations it becomes clear that changing the stiffness has an effect on the stability, but if this is due to the flap-lag-stall instability or due to the edgewise instability is not clear. The effect of the reduction of the difference between the first flap and first lag frequency does not always lead to a reduction in the damping, sometimes and increase in the damping is observed.

Notations

A	= Energy of mass matrix
E	= Young's modulus
G	= Modulus of elasticity in shear
I_p	= Polar moment of inertia
I_β, I_ς	= Area moment of inertia about flap/lag axis
k	= Partitioning coefficient
k_β k_ς	= Spring stiffness flap/lag
p	= Generalised momentum
q	= Generalised coordinate
Q	= Generalised force
T	= Kinetic energy
V	= Potential energy
$\bar{\omega}$	= Non-dimensional eigenfrequency

1. Introduction

In a world where the energy use keeps rising and the devastating effects on the environment of oil burning generators is becoming clear, wind energy is one of the alternatives to provide clean energy. To supply more clean energy, the wind turbines have, over the years, become larger and more powerful. Small wind turbines up to 60 meters in diameter did not appear to suffer from aeroelastic instabilities. However, larger wind turbines have sometimes shown devastating aeroelastic instabilities. It is therefore important to understand these instabilities and to prevent them from occurring in new turbines. In ref [1,2] it was concluded that one of the possible problems was the so-called flap-lag-stall, which can sometimes occur in wind turbines, especially in large wind turbines. The possibility of this instability is due to the method used to scale up the turbines [3]. The scaling brings the flap and lead-lag frequencies closer together. This combined with operating close to stall results in a possible instability. At the same time it is always possible for a wind turbine operating close to stall to experience negative damping in edgewise direction due to the aerodynamic forces (ref [4]). In an attempt to further investigate the flap-lag-stall instability and the difference between this instability and the edgewise instability, this paper looks at the stability of a single blade with normal stiffness and compares this with blades with reduced lag stiffness and blades with increased flap stiffness. This way the flap- and lag frequency come closer together than in the original blade and the stability could therefore be reduced due to the flap-lag stall instability, given that the turbine operates close to stall. To investigate the stability of these different blade models, time simulations have been performed using a fully nonlinear rigid body simulation tool. These are then analysed using a system identification tool.

The background of this research will be sketched in chapter 2, where the flap-lag-stall instability and the edgewise instability are described. Chapter 3 will shortly discuss the programme that has been used to perform the simulations. The model that has been used to analyse the instability is shown in chapter 4 while chapter 5 describes the post-processing method used to get from the time series that result from the simulations to damping coefficients. Finally, in chapter 6 the results are shown and discussed after which the last chapter will give the conclusions.

2. Instabilities

2.1 Flap-Lag-Stall Instability
The instability observed in some large wind turbines has not been observed in smaller wind turbines.

Therefore it can be expected that the instability is scale dependent. After a literature survey [5] and analysing the scale dependency of instabilities it was concluded that one of the possible instabilities was due to the method used in scaling the blades. The scaling of the blades is performed in such a way that the lead-lag and flap frequencies come closer together. These frequencies are usually calculated for clamped blades. Also when the frequencies are measured, this is often done trying to clamp the blade with infinite stiffness. In reality however, different eigenmodes for two or three bladed rotors can reduce the lead-lag frequency even more [3]. If the hub rotates as part of the eigenfrequency, this will in fact decrease (or increase, depending on the direction) the lag frequency. Therefore these frequencies are then even closer together then the measurements or calculations might suggest. This is illustrated in figure 1.
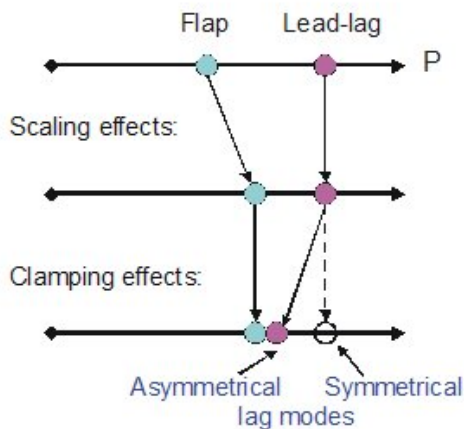
Figure 1: Flap and Lag frequencies approach each other

For helicopters is has been shown that the flap-lead-lag instability will only occur if the rotating flap eigenfrequency is between $1.0 < \bar{\omega} < \sqrt{2}$ [6]. For wind turbines, the flap frequency will be much higher than this (e.g for the turbine used in this paper it is appr. 3.5). From this one would expect no problem with instabilities for a wind turbine due to these two frequencies being close. However, by analysing a simple single blade model, it has been found that this instability might still occur due to the influence of stall [1,3,7,8]. When the lift behaviour becomes nonlinear, but even before that, when the drag becomes progressively larger, the stabilising aerodynamic torque variations become smaller and the destabilising Coriolis-forces can become more dominant. In that case the flap-lag-stall instability is possibly a dangerous problem. As it can occur before lift stall occurs, when the drag increases rapidly ("drag-stall"), it is assumed that drag-stall will be most critical.

The motion for this instability will mainly be a lead-lag motion. There can be some flapping motion, but the lead-lag motion will be dominant. These large lead-lag motions of the blades will excite tower motions. The tower motions that result in large translational movements of the rotor centre will be excited most by the vibrating blades. If the frequency relationship between the flap-lag-stall instability and one of these tower modes is unfavourable, the tower will act as a dynamic vibration absorber. This can result in large amplitude motions of the tower where the flap-lag-stall instability is the energy source for this tower instability [9].

2.2 Edgewise Instability in Stall

Another instability that can occur in large stall-regulated wind turbines is an instability in edgewise direction caused by negative aerodynamic damping for the in-plane vibration [4]. This occurs for angles of attack close to stall. The lift coefficient c_l and the derivative of the drag coefficient $\dfrac{dc_d}{d\alpha}$ will both always give negative contributions to the aerodynamic damping for in-plane vibrations in a stall-regulated wind turbine. Only the drag coefficient will give a positive contribution to the aerodynamic damping.

The structural pitch angle defining the stiffest and most flexible directions of the blade, plays an important role in preventing this instability. The out-of-plane vibration will be strongly damped. If the lead-lag eigenmode has components in the out-of-plane direction, this will aid the damping for this mode.

This edgewise instability will also lead to increasing vibrations in the lead-lag direction, just like the flap-lag-stall instability discussed in the previous section.

3. WOBBE, a Fully Nonlinear Simulation Tool

The tool used to perform the simulations of the single blade model is called WOBBE. It is a fully nonlinear rigid body simulation tool. This chapter will give a very brief description of the tool, for more information the interested reader is referred to ref. [10].

WOBBE can simulate rigid body systems, where the bodies are interconnected by hinges and springs (fig 2) with aerodynamic forces acting on the system. The tool can be used for many different systems, but the development is currently concentrating on wind turbines and helicopters. Hamiltonian dynamics are used to find the equations governing the motions of the system. The state variables used in WOBBE are the generalised coordinates (angles) q_i and

Hamilton's generalised momentum $p_i = \dfrac{\partial T}{\partial \dot{q}_i}$. The generalised coordinates are illustrated in figure 2.

The kinetic energy T of a system such as shown in figure 2, can be written as a homogenous quadratic function of the velocities:

$$T = \tfrac{1}{2}\vec{\dot{q}}\,\overline{\overline{A}}\,\vec{\dot{q}} \qquad (3.1)$$

where A is the energy matrix. This matrix depends only on the generalised coordinates and properties of the different elements, as described in ref [10].
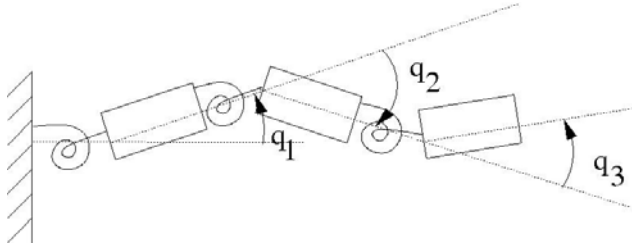
Figure 2: The generalised coordinates in WOBBE

Differentiating this equation to find the generalised momentum results in:

$$\frac{\partial T}{\partial \vec{\dot{q}}} = \overline{\overline{A}}\,\vec{\dot{q}} = \vec{p}$$

$$(3.2)$$

From this equation it is possible to calculate the angular velocities $\vec{\dot{q}}$ by inverting the matrix A, once Hamilton's generalised momenta $\vec{p}$ are known.

Once these velocities $\vec{\dot{q}}$ are known, the time derivatives of Hamilton's generalised momenta can be calculated using Lagrange's equations:

$$\dot{p}_i = \frac{\partial T}{\partial q_i} - \frac{\partial V}{\partial q_i} + Q_i \qquad (3.3)$$

where V is the potential energy from the springs and gravitational forces and Q_i is the generalised force due to the aerodynamics acting on the system. The calculations are summarised in figure 3. This shows that given the generalised coordinates and generalised momentum at a certain time step it is possible to calculate the energy matrix and the angular velocities of the generalised coordinates.

Figure 3: Flow Diagram of WOBBE
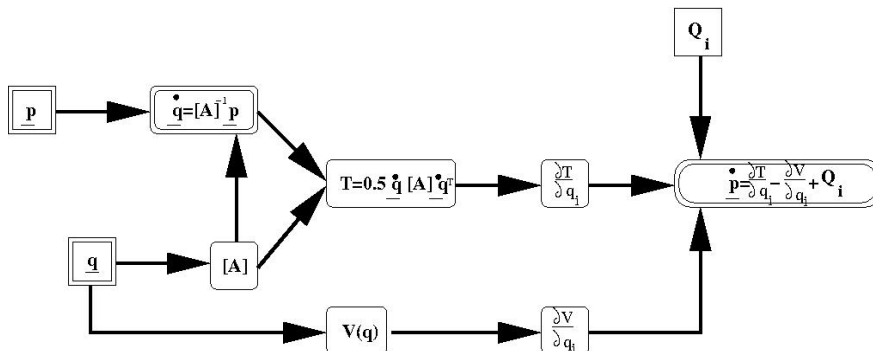
The potential energy depends on the generalised coordinates and the derivative of the kinetic energy can be determined once the velocities are known. The velocities and generalised coordinates also determine the inflow at the different aerofoils and therefore the generalised forces. So it is possible to calculate the time derivatives of both state variables. Integration will result in fully nonlinear simulation results.

To determine the aerodynamic forces in WOBBE, use is made of the blade element momentum theory. The induction factor a is calculated over the entire rotor plane and assumed constant over this rotor plane. The variation in time of the induced velocity is simulated using a dynamic inflow model. This is done not only because this is more realistic, but also because it does not necessitate an extra iteration to find the induced velocity. For the simulations discussed in this paper quasi-steady aerodynamics have been used, but it would also have been possible to use the implemented model for unsteady aerodynamics.

The output data from WOBBE are the generalised coordinates at the different time steps. It is also possible to create an output file containing the positions of the hinges relative to the rotor hub in the rotating reference frame at the different time steps, which can be very useful when using a detailed model, as this will then show the lower eigenfrequencies more clearly. The power output, induction factor and thrust coefficient are also given at the different time steps as are the angles of attack at the beginning of the different rigid bodies.

4. Model with 15 degrees of freedom

The model of the single blade is based on an actual wind turbine blade of 40 meters radius. The blade is part of a variable speed wind turbine. However, as the instabilities under investigation mainly occur close to stall, the configuration that would result in an active stall regulated wind turbine is used.

The blade is divided into three so-called superelements [11,12]. One superelement consists of four rigid bodies as shown in figure (4) with a total of five degrees of freedom. The different rigid bodies are connected by torsional springs. The length of the two rigid bodies in the middle is (½ - k)L, as shown in the figure. L is the length of one superelement and k is the partitioning coefficient (0<k<½). The other two elements are both kL long. Rauh [11] concludes that choosing this partitioning coefficient influences the results and when the value of k is

57.3

between 0.2 and 0.25 the exact eigenfrequencies are approximated using only a limited number of superelements. Furthermore for $k = \frac{1}{2}(1 - \frac{1}{\sqrt{3}}) \approx 0.211$ the spring stiffness of the spring between the first and last element becomes zero [13]. For this reason, this value of k will be used in the models of wind turbines in WOBBE.

The first element of a superelement is clamped. Therefore the last element of one superelement will form a rigid body with the first element of the following superelement. This results in an element with a length that is *2kL* as shown in figure (4).

The stiffnesses of the springs are chosen such that for a uniform beam the deformation and the slope at the tip of the beam will be equal to the values of a theoretical beam in pure bending. For this model of a blade the stiffness is calculated by averaging the stiffness of the blade over the length of one superelement. For the flap and lag springs in one superelement the equations used are [13]:

$$k_\beta = \frac{2(\overline{EI}_\beta)}{L}; \quad k_\varsigma = \frac{2(\overline{EI}_\varsigma)}{L} \qquad (4.1)$$

where k_β is the stiffness in the most flexible direction (flap) and k_ς the stiffness in the stiffest direction (lead-lag). The bar over *EI* means that the average over the length of the superelement *L* is taken. Therefore the two lag springs and the two flap springs in one superelement will have equal stiffness. A spring in another superelement will have another value for its stiffness.

The torsion spring is calculated using:
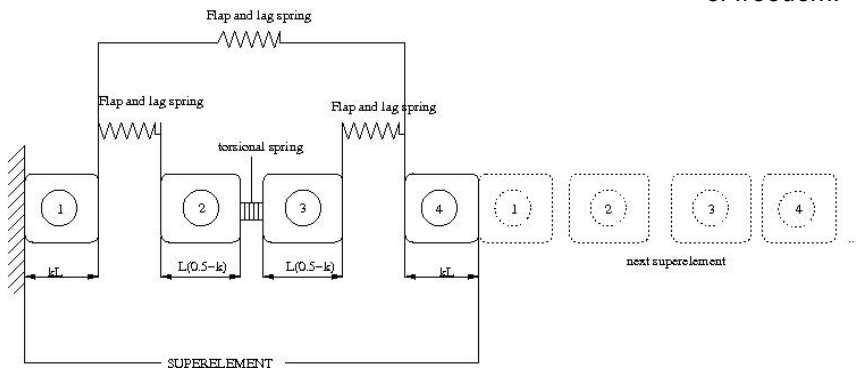
$$k = \frac{\overline{GI}_p}{L} \qquad (4.2)$$

again taking the average stiffness over the length of the superelement.

Figure 4: One superelement consisting of four rigid bodies

The first part of a wind turbine blade will always be very stiff compared to the rest of the blade, especially when the hub is modelled as part of the blade. This part of the blade has to be assumed infinitely stiff and the stiffness cannot be included in the calculation of the springs (Eq. 4.1). The calculation of the spring stiffness therefore starts after the extremely stiff part of the blade. Considering that the first element of the first superelement will be clamped, this will also become part of the first rigid body as depicted in figure 4. All superelements in the blade have the same length *L*.

15 Degrees of freedom: 6 flap, 6 lag and 3 torsion
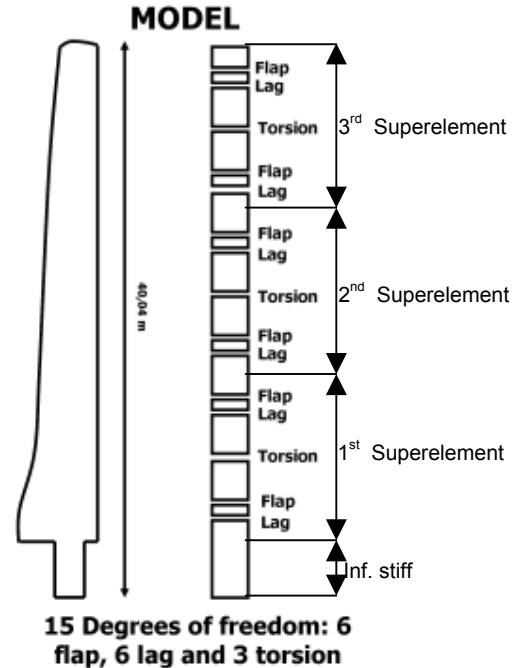
Figure 5: Model of the single blade with 15 degrees of freedom.

The flap and lead-lag hinges should be in the same place. However within WOBBE it is possible to give every element only one degree of freedom, therefore the two hinges must be connected to two different elements. It is possible to use elements with zero mass, length etc, but this can sometimes result in numerical problems. For this reason every element behind the flap and lag springs are divided into two rigid bodies. The first element is behind the lag hinge and is only 1% in length of the total element. The flap hinge comes after this small rigid body followed by the rest of the element. This means that the model used consists of 16 elements with a total of 6 flap, 6 lead-lag and 3 torsional degrees of freedom as shown in figure 5. The first element will rotate at a constant rotational speed.

The mass and inertia of the elements are calculated by determining the mass and inertia of the actual sections of the blade, so no averages are used for this. The structural pitch however is taken as an average over the length of one superelement. This angle determines the stiffest and most flexible direction of the blade. It is not possible to use any coupling terms between the different stiffnesses in WOBBE, therefore the hinges must be in the principal directions of the blade. There can be a difference in the principal directions of different superelements. The pitch setting of the blade is added to the structural pitch angle of the first superelement.

The chord and thickness ratio of the elements are assumed to be linear between the beginning and end of an element. The values of these properties at these two points on one element are the same as the actual values at these points on the real blade. Structural damping is not taken into account. Therefore all results will show less damping then in reality.

To investigate the effect of changing the difference between the first flap and first lead lag frequency of the blade, the simulations were run with five different blade models:

Model	Description, relative to original blade
A	Original blade
B	Reduction of lag stiffness, difference between flap and lag reduced by 75%
C	Reduced lag stiffness to equal flap stiffness
D	Increased flap stiffness, difference between flap and lag reduced by 75%
E	Increased flap stiffness to equal lag stiffness

Table 1: Different models simulated using WOBBE

Ad. B): The new value of the springs in the lead-lag hinges therefore become:

$$k_{\varsigma_{75}} = k_\varsigma - (k_\varsigma - k_\beta) \cdot 0.75 \qquad (4.3)$$

and similar to this for D:

$$k_{\beta_{75}} = k_\beta - (k_\beta - k_\varsigma) \cdot 0.75 \qquad (4.4)$$

The simulations were run for configurations for 5 m/s, 8 m/s, 12 m/s, 15 m/s and 18 m/s. For each wind speed a certain pitch setting and rotational velocity is used. As mentioned before, these settings are not the actual settings of the wind turbine, but of a model of an active stall regulated wind turbine that results in the same power for the different wind speeds as the actual wind turbine.

Every simulation is preceded by an initial simulation that is used to determine the average values of the generalised coordinates for the given wind speed and configuration. These average values determine

the steady state of the blade for the specific configuration and wind speed. The simulation used for analysis is then started close to the steady state. For very small deviations from the steady state, the results of the simulations will become linear.

Because the flap vibration will be strongly damped, the amplitudes given to the flap angles are larger than the other angles. If these angles are taken too small, the flap vibration will not be identified correctly, because the flap vibration will hardly be present in the simulation results. The linearity of the results is checked using the identification method described in the next chapter.

5. Processing the results

As mentioned in chapter 3 of this paper, the simulation tool used to perform the simulations is fully nonlinear. For this reason the results do not clearly show (in)stabilities. Post-processing of the results is required to gain quantative results. When the simulations are performed using very small deviations of the equilibrium positions, the results become (nearly) linear and therefore it is then possible to find quantative results that can be compared to each other. Fully nonlinear results on the other hand will not actually give one damping coefficient for each eigenfrequency. The damping will depend on the amplitude which in turn will be changing in time. This makes it very difficult to compare nonlinear results quantatively. FFT can be used to analyse the results (filtering or moving block), but as there is not really one unique value for the damping, it is possible to easily manipulate these results. It is also very difficult to perform this method consequently to get results that can be compared.

For this reason, in order to find quantative results, small deviations from the equilibrium positions are wished for. That way the results are (almost) linear and can be used in a linear identification tool. To find the damping, the system identification tool AerID is used [14]. By identifying the linear system corresponding to the time response from WOBBE, the eigenfrequencies and the corresponding damping coefficients can be determined.

To check if the results are linear, it is possible to run another simulation with half the amplitude at the start of the simulation. The system that is identified from the original simulation can be used to investigate the linearity of the results. Multiplying the identified response by 0.5 and comparing this to the results obtained by WOBBE for the smaller amplitude shows the linearity of the system. The results of such a process are shown in figure 6 for model C at 18 m/s. If the identification was successful and the amplitudes are small enough, the identified result coincides with the results obtained from the second
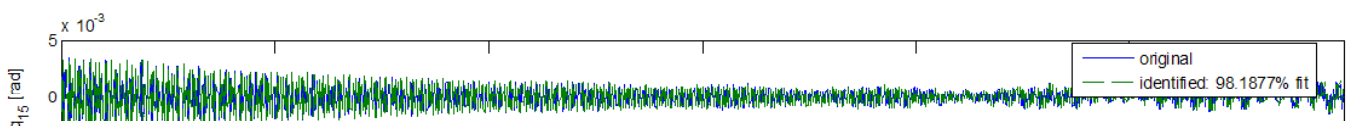
Figure 6: Check of the linearity of the result. In this case of the last flapping angle in the model, for model C at 18 m/s.

simulation using half the amplitudes. For the example given, this was clearly the case. A perfect correspondence will not quickly occur, also because the steady state is not predicted exactly and the amplitudes are small relative to this steady state. Therefore small deviations in the calculation of the steady state will cause larger differences in the identified amplitude.

The results of the linear identification of the original simulation will also indicate if they are linear or not. If the tool is not able to identify the response very well, the reason often is that the response is not yet linear. If the identification corresponds very well to the results from WOBBE, then these results must be linear.

When a configuration becomes unstable, the amplitudes will grow, therefore it will become nonlinear after some time. For these cases it can be very hard to obtain good results. Often a shorter time span has to be used to find results that remain more or less linear. For the calculations described in this paper, this was the case for all configurations at 18 m/s. For this reason the simulations of the different configurations at 18 m/s only ran for 30 seconds, while all other simulations were for a duration of 50 seconds.

An iterative process has been used to obtain linear results for all simulations. For the low wind speeds, it was always obtained easily by using the same amplitude for all configurations. For higher speeds, the results became unstable. Therefore it was harder to find responses that were close enough to linear to result in a useful identification. By cutting the time span for the 18 m/s simulations it was possible to obtain good results for all simulations.

6. Results

The simulations were all successfully run and identified. The lead-lag frequency changed due to the change in the stiffness of the springs for configurations B and C. For configurations D and E the flap eigenfrequency changed. The frequencies for the different configurations at the different wind speeds were determined by the identification tool and are shown in table 2 and table 3.

The frequencies are also illustrated in figure 7 and 8. The tables also show that the flap and lead-lag frequencies do not exactly coincide for blades C and E. For these blades the stiffness in lead-lag direction and flap direction have been equalised. The difference in the frequencies is due to the difference in centrifugal stiffening for the flap and the lead-lag mode. There is also a difference in the moments of inertia about the flap and lead-lag axis, which will also result in a difference between the frequencies if springs of equal stiffness are chosen.

Changing the lead-lag or flap stiffness does not only change the eigenfrequencies. It also results in changes in a.o. the steady state. The effect on the angle of attack is very small. The average value of the angle of attack does not show a change, as illustrated in figure 9. The amount of variation in angle of attack does show differences.

The identified damping for the first flap mode is shown in figure 10 and for the first lead-lag mode the damping is shown in figure 11. Figure 10 shows that the damping of the first flap mode is unchanged i the cases where the lead-lag stiffness is changed and it show a decrease for the cases where the blade's flap stiffness has been increased. Figure 11 shows that the wind turbine blade suffers from instabilities in its base model. The configuration of the stall regulated turbine has been chosen to result in the same power as the original pitch regulated variable speed turbine. This has resulted in a model that becomes unstable for some wind speeds in the first lead-lag mode. For the cases calculated in this paper the highest two wind speeds (15 m/s and 18 m/s) show the blade to be unstable. However, if the structural damping would be taken into account, this instability will probably disappear.

Figure 11 also shows a very small decrease in stability for all blades compared to the baseline blade (A) for 5 and 8 m/s, but an increase for 12 and 15 m/s. This trend cannot yet be explained. A more detailed investigation of the results is needed.

It also shows that the stabilising effect is greatest for blades C and E, these are the blades where the stiffnesses in flap and lead-lag direction have been set equal to each other and therefore the eigenfrequencies of the first two modes are very close.

Model \ wind speed	5	8	12	15	18
A	0.99	1.04	1.04	1.04	1.03
B	0.98	1.04	1.04	1.03	1.03
C	0.98	1.03	1.03	1.04	1.03
D	1.75	1.78	1.77	1.76	1.76
E	1.91	1.93	1.93	1.95	1.94

Table 2: Identified first flap frequencies for the different models at the different wind speeds.

Model & freq. \ wind speed	5	8	12	15	18
A	1.89	1.89	1.89	1.89	1.89
B	1.37	1.38	1.38	1.38	1.38
C	0.96	0.98	0.98	0.97	0.98
D	1.89	1.90	1.90	1.91	1.90
E	1.89	1.90	1.90	1.88	1.89

Table 3: First lead-lag frequencies for the different models at the different wind speeds.
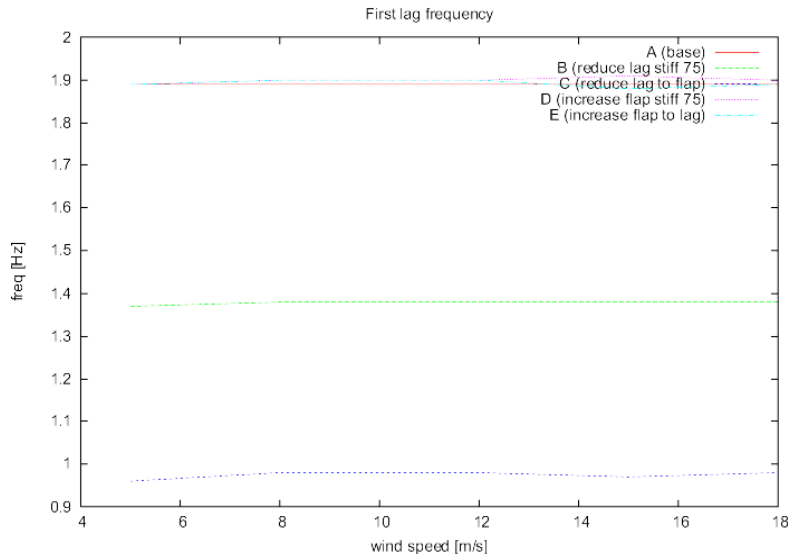
Figure 7: First flap frequencies of the different blades
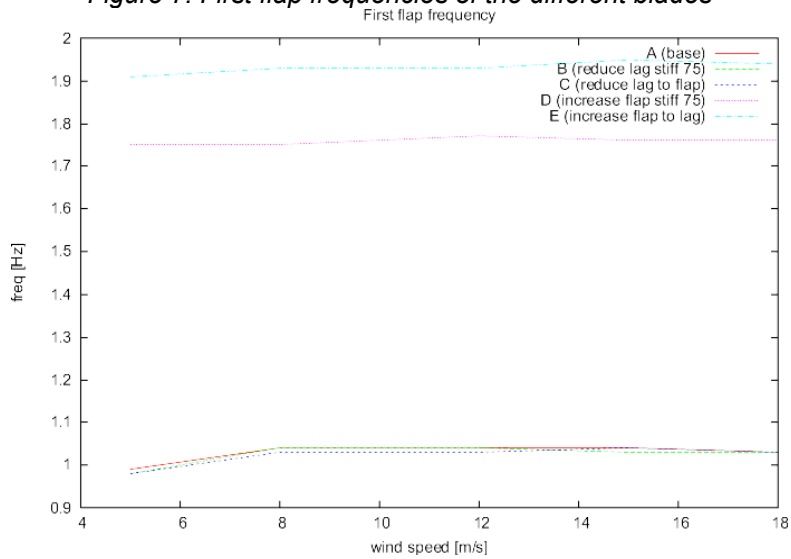
Figure 8: First lead-lag frequencies of the different blades
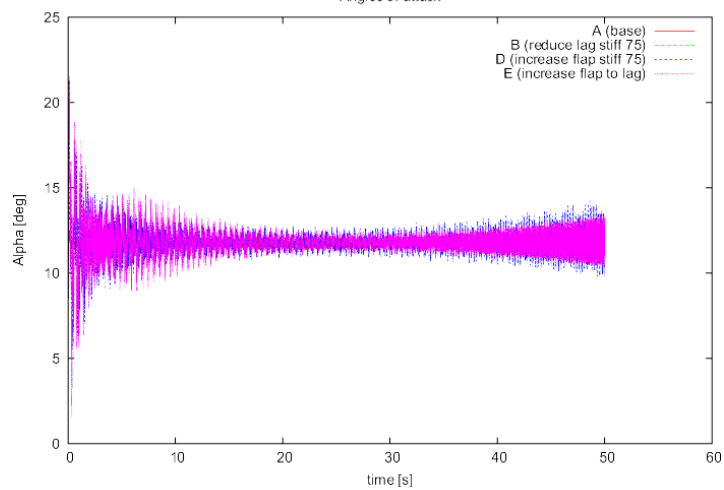
Figure 9: The behaviour in time of the angles of attack at a point on the blade, for three different blades, all at 15 m/s.

The time series resulting from the simulations show the instabilities at the higher wind speeds very clearly. The difference between the different models also appears very clearly in these results. This is illustrated in figure 12. This figure shows the time series of the 6th generalised coordinate for simulations at 18 m/s. Note that the different simulations were not all run starting from the exact same amplitudes relative to the steady state. The difference in steady state is clearly visible and the difference between blade C (weakest instability) and blade E (strongest instability) is also clearly illustrated.

7. Conclusions

The simulations of the wind turbine blade showed that changing the lead-lag stiffness while keeping the flap stiffness the same does not influence the damping of the first flap mode. Only for a wind speed of 15 m/s a small difference shows up.
The damping of the first lead-lag mode becomes slightly smaller for the low wind speeds, but it improves for higher wind speeds (up to 15 m/s), where the baseline blade has become unstable. The altered blades are also unstable, but the damping is less negative than the damping of the baseline blade. This effect is greatest for the two blades where the first flap and first lag frequency almost coincide.
A closer look at the two instabilities is necessary to find out if the flap-lag-stall instability can actually occur before the edgewise instability and if the flap-lag-stall instability is a real danger or that the edgewise instability will be the most critical one and the coincidence of the flap and lead-lag frequency is not important for the stability of the blade. The flap-lag-stall instability has not yet clearly shown up during this investigation, but from the analyses it has also not become clear which instability is actually occurring. Both instabilities will result in increasing vibrations in the lead-lag direction. From analysis it becomes clear that this is the case for the analysed blades at higher wind speeds. But it cannot easily become clear which instability the blade is suffering from.
Next to this, if the flap-lag-stall instability is a danger, a quantification should be determined on how close the first flap and first lag frequency should be for this instability to become a danger. The same goes for the proximity of the flap frequency to the rotational frequency of the turbine. It was concluded that the limit found in helicopter is not valid in wind turbines, but it is possible that the flap frequency of this blade is too high compared to the rotational frequency for the flap-lag-stall instability to occur.

All in all changing the blade stiffness which results in frequencies coming closer together did not result in a clear trend that was expected.

References

[1] J.G. Holierhoek, Th. van Holten, Th.J. Mulder, "Automatic Simulation to Determine the Aeroelastic Stability of Large Scale Wind Turbine Rotors (With Emphasis on Flap-Lag-Stall Flutter)", *Proceedings of the 26th European Rotorcraft Forum, The Hague the Netherlands, 26-29 September 2000,* paper no. 69
[2] Th. van Holten, M.D. Pavel, G.N. Smits, "The Influence of Scale Effects on the Aeroelastic Stability of Large Wind Turbines", P*roceedings of the 26th European Rotorcraft Forum, The Hague the Netherlands, 26-29 September 2000,* paper no. 71.
[3] Th. van Holten, J.G. Holierhoek, "The Influence of Scale Effects on the Aeroelastic Stability of Large Wind Turbines", *Proceedings of International Forum on Aeroelasticity and Structural Dynamics 2001, IFASD 2001,Madrid Spain, 5-7 June*, Vol. III, pp.53-64.
[4] J.T. Petersen e.a., Prediction of Dynamic Loads and Induced Vibrations in Stall, Risø-R-1045(EN), May 1998, Risø National Laboratory, Roskilde, Denmark
[5] M.D. Pavel and M.M.J. Schoones, *Literature Survey on Aeromechanical Instabilities for Helicopters and Wind Turbines, STABTOOL: Phase 3*, Memorandum M-877, July 1999, Faculty of Aerospace Engineering, Delft university of Technology
[6] R.A. Ormiston and D.H. Hodges, *Linear Flap-Lag Dynamics of Hingeless Rotor Blades in Hover*, Journal of the American Helicopter Society,17:2, April 1972
[7] J.G. Holierhoek, Th. van Holten, "Flap-Lag Instability of Large Wind Turbines", *European Wind Energy Conference,* Copenhagen, Denmark, 2001 paper no. PG2.2.
[8] Th. van Holten and J.G. Holierhoek , "The Influence of Scale Effects on the Aeroelastic Stability of Large Wind Turbines", *European Wind Energy Conference*, Copenhagen, Denmark, 2001, paper no. OC4.1.
[9] J.G. Holierhoek, Th. van Holten, Th.J. Mulder, "Aeroelastic Stability of Large Wind Turbines (With Emphasis on Flap-Lag Flutter)", *4th GRACM*

Congress on Computational Mechanics, Patras, Greece, 2002.

[10] K. van Overbeek, Th. van Holten, "Automatic Simulation of Complex Non-Linear Dynamic Systems", *Proceedings of the 26th European Rotorcraft Forum, The Hague the Netherlands, 26-29 September 2000,* paper no. 65.

[11] J. Rauh, *Ein Beitrag zur Modellierung elastischer Balkensysteme*, Fortschritt-Berischte VDI, VDI-Verlag GmbH, Düsseldorf, Reihe 18: Mechanik/Bruchmechanik, 37, 1989

[12] J. Rauh and W. Schiehlen, *Various Approaches for the Modeling of Flexible Robot Arms*, Proceedings of the Euromech-Colloquium 219 on Refined Dynamical Theories of Beams, Plates, and Shells and their Applications, pages 420--429, 1986

[13] D.P. Molenaar, *Cost effective design and operation of variable speed wind turbines*, DUP Science, Delft, The Netherlands, 2003

[14] B. Marrant, P. Lisandrin, Th. van Holten, "Aero-elastic Analysis of Wind Turbines using System Identification Techniques", *Proceedings of the 31st European Rotorcraft Forum, Florence, Italy, 13-15 September 2005*, paper no. 58.
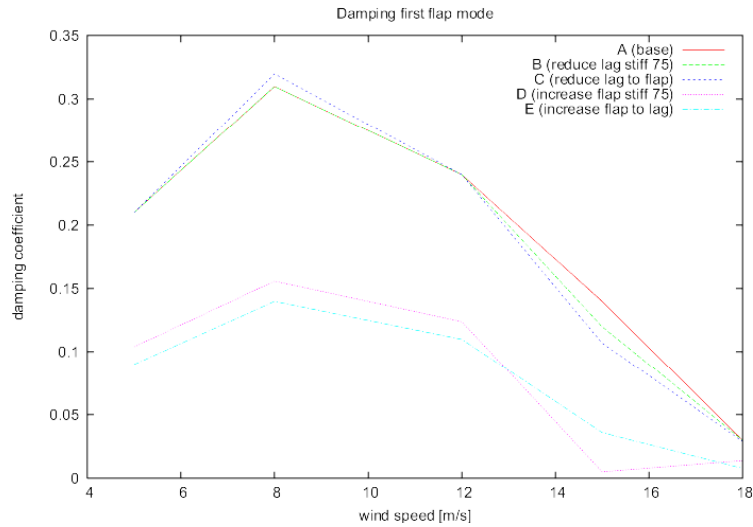
Figure 10: Damping of the first flap mode for different wind speeds and different blades.
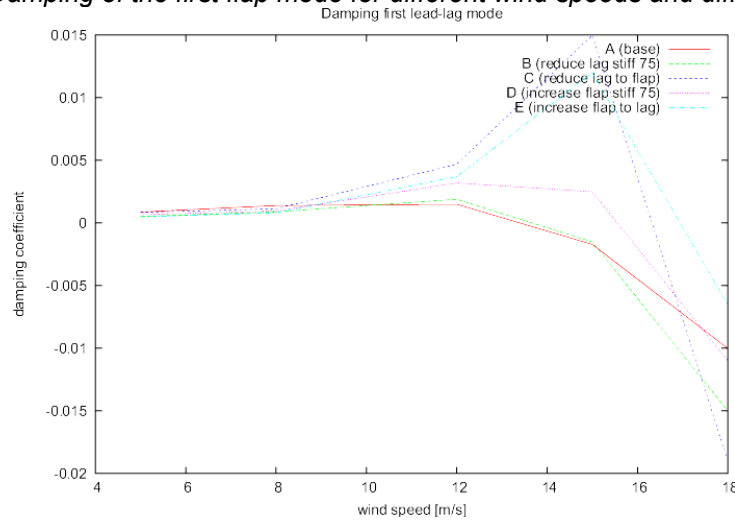
Figure 11: Damping of the first lead-lag mode for different wind speeds and different blades
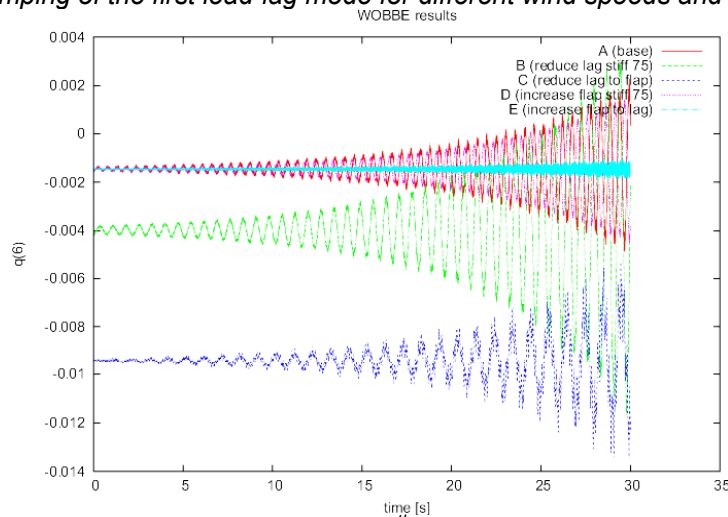
Figure 12: Time response resulting from WOBBE for the 6th degree of freedom (lead-lag) for the different blades at 18 m/s. The starting amplitude was not the same for all blades.

57.10